THE JOURNAL OF BIOLOGICAL CHEMISTRY
Vol. 278, No. 33, Issue of August 15, pp. 31118–31127, 2003
Printed in U.S.A.

Heparan Sulfate 6-*O*-Sulfotransferase Is Essential for Muscle Development in Zebrafish*

Received for publication, December 23, 2002, and in revised form, May 28, 2003
Published, JBC Papers in Press, June 1, 2003, DOI 10.1074/jbc.M213124200

Robert J. Bink,[a,b,c] Hiroko Habuchi,[c,d] Zsolt Lele,[c,e] Edward Dolk,[a,f] Jos Joore,[a,g] Gerd-Jörg Rauch,[h,i] Robert Geisler,[h] Stephen W. Wilson,[e] Jeroen den Hertog,[a] Koji Kimata,[d] and Danica Zivkovic[a,j]

From the [a]Hubrecht Laboratory, Netherlands Institute for Developmental Biology, Uppsalalaan 8, 3584 CT Utrecht, the Netherlands, the [d]Institute for Molecular Science of Medicine, Aichi Medical University, Nagakute, Aichi 480-1195, Japan, the [e]Department of Anatomy and Developmental Biology, University College London, Gower Street, London WC1E 6BT, United Kingdom, and the [h]Max-Planck-Institut für Entwicklungsbiologie, Abteilung III-Genetik, Spemannstrasse 35, 72076 Tübingen, Germany

Heparan sulfate proteoglycans function in development and disease. They consist of a core protein with attached heparan sulfate chains that are altered by a series of carbohydrate-modifying enzymes and sulfotransferases. Here, we report on the identification and characterization of a gene encoding zebrafish heparan sulfate 6-*O*-sulfotransferase (*hs6st*) that shows high homology to other heparan sulfate 6-*O*-sulfotransferases. When expressed as a fusion protein in cultured cells, the protein shows specific 6-*O*-sulfotransferase activity and preferentially acts on the iduronosyl *N*-sulfoglycosamine. In the developing embryo, *hs6st* is expressed in the brain, the somites, and the fins; the same structures that were affected upon morpholino-mediated functional knockdown. Morpholino injections significantly inhibited 6-*O*- but not 2-*O*-sulfation as assessed by HPLC. Morphants display disturbed somite specification independent of the somite oscillator mechanism and have impaired muscle differentiation. In conclusion, our results show that transfer of sulfate to specific positions on glycosaminoglycans is essential for muscle development.

Heparan sulfate proteoglycans (HSPGs)[1] are macromolecules with divergent structures and functions. They are located on the cell surface and in the extracellular matrix and are composed of a core protein to which highly sulfated glycosaminoglycan (GAG) sugar chains are attached. Heparan sulfate (HS) is a GAG of repeating disaccharide subunits that consists of glucosamine and glucuronic/iduronic acid and is modified in a complex series of steps involving deacetylation, sulfation, and epimerization (1). In each of these modification steps only part of the substrate is modified resulting in a high sequence diversity, which is thought to give HSPGs their functional specificity and versatility. HSs specifically bind to various extracellular molecules including growth factors, adhesion molecules, proteases, and receptors to regulate cell proliferation and differentiation during various developmental processes (2).

In *Xenopus* ectodermal explants, removal of GAGs from proteoglycans by heparinase results in inhibition of elongation and mesodermal differentiation in response to activin, FGF, and Wnt (3). Similar experiments in cockroach embryos perturbed the directed growth of axon pioneer fibers (4). In vertebrates, this function is conserved as it has been shown that exogenous addition of heparan sulfate causes misrouting of retinal axons at the tectal border (5). Recently, this misrouting of axon targeting was attributed to inhibition of sulfation of heparan sulfate (6). The zebrafish mutant *knypek* (*kny*) displays impaired convergent extension movements and the gene responsible for the mutant phenotype encodes a member of the glypican family of HSPGs. Kny is involved in the non-canonical Wnt/planar cell polarity pathway enhancing Wnt11 signaling in overexpression experiments and the *kny* mutation exacerbates the convergent extension defect of *silberblick*(*slb*)/*wnt11* mutants (7). Genetic screens in *Drosophila* have yielded the *sugarless* (*sgl*) and *sulfateless* (*sfl*) mutants that are involved in HSPG biosynthesis as they encode UDP-glucose dehydrogenase and heparan sulfate *N*-deacetylase/*N*-sulfotransferase, respectively (8, 9). Their pleiotropic mutant phenotypes suggest that they have diverse functions in fibroblast growth factor

* This work was supported by the German Human Genome Project (DHGP Grant 01 KW 9919) and the National Institutes of Health (NIH Grant 1 R01 DK55377-01A1) (to R. G.). The costs of publication of this article were defrayed in part by the payment of page charges. This article must therefore be hereby marked "*advertisement*" in accordance with 18 U.S.C. Section 1734 solely to indicate this fact.

The nucleotide sequence(s) reported in this paper has been submitted to the GenBank™/EBI Data Bank with accession number(s) AJ505990.

[b] Present address: Netherlands Forensic Institute, Volmerlaan 17, 2288 GC Rijswijk, the Netherlands.

[c] These authors contributed equally to the work.

[f] Present address: Dept. of Molecular Cell Biology, University Utrecht, Padualaan 8, 3584 CH Utrecht, the Netherlands.

[g] Present address: Pepscan Systems, Edelhertweg 15, 8219 PH Lelystad, the Netherlands.

[i] Present address: Dept. of Developmental Biology, Stanford University School of Medicine, Stanford, CA 94305.

[j] To whom correspondence should be addressed. Tel.: 31-30-2121800; Fax: 31-30-2516464; E-mail: dana@niob.knaw.nl.

[1] The abbreviations used are: HSPG, heparan sulfate proteoglycan; HS, heparan sulfate; *hs6st*, heparan sulfate 6-*O*-sulfotransferase; mHS6ST, mouse HS6ST; HS2ST, heparan sulfate 2-*O*-sulfotransferase; $GlcNSO_3$, *N*-sulfoglucosamine; $GlcNSO_3(6SO_4)$, *N*-sulfoglucosamine 6-sulfate; IdoUA-$(2SO_4)$, iduronic acid 2-*O*-sulfate; ΔDi-OS, 2-acetamide-2-deoxy-4-*O*-(4-deoxy-α-L-*threo*-hex-4-enepyranosyluronic acid)-D-glucose; ΔDi-6S, 2-acetamide-2-deoxy-4-*O*-(4-deoxy-α-L-*threo*-hex-4-enepyranosyluronic acid)-6-*O*-sulfo-D-glucose; ΔDi-NS, 2-deoxy-2-sulfamino-4-*O*-(4-deoxy-α-L-*threo*-hex-4-enepyranosyluronic acid)-D-glucose; ΔDi-(*N*,6)diS, 2-deoxy-2-sulfamino-4-*O*-(4-deoxy-α-L-*threo*-hex-4-enepyranosyluronic eg acid)-6-*O*-sulfo-D-glucose; ΔDi-(*N*,2)diS, 2-deoxy-2-sulfamino-4-*O*-(4-deoxy-2-*O*-sulfo-α-L-*threo*-hex-4-enepyranosyluronic acid)-D-glucose; ΔDi-(*N*,6,2)triS, 2-deoxy-2-sulfamino-4-*O*-(4-deoxy-2-*O*-sulfo-α-L-*threo*-hex-4-enepyranosyluronic acid)-6-*O*-sulfo-D-glucose; PAPS, 3′-phosphoadenosine 5′-phosphosulfate; CDSNS-heparin, completely desulfated and *N*-resulfated heparin; NS-heparosan, deacetylated, and *N*-sulfated heparosan; CDSNAc-heparin, completely desulfated *N*-acetylated heparin; EHS, Engelbreth-Holm-Swarm; GAG, glycosaminoglycan; HPLC, high performance liquid chromatography; hpf, hours post fertilization.

(FGF) and Wnt signaling (8, 9). Similarly, examination of the *Drosophila tout-velu* mutant and the *Ext1*-deficient mouse, that both lack heparan sulfate co-polymerase, indicate that HSPGs are essential for Hedgehog signaling (10, 11, 12). Recently, it has also been demonstrated that the heparan-specific sulfatase, QSulf1, alters the sulfation state of GAGs, which in turn regulate Wnt signaling (13).

One major challenge in understanding the function of various HSPGs in development is to clarify the specific role the different side-chain modifications play in altering their function. The importance of number and position specificity of sulfate groups on heparan sulfate is demonstrated by the mouse heparan sulfate 2-*O*-sulfotransferase knock-out that exhibits renal, eye, and skeletal defects (14), and by mice lacking proper *N*-deacetylase/*N*-sulfotransferase-1 function resulting in pulmonary hypoplasia, atelectasis and respiratory distress syndrome (15).

Here we report the cloning and characterization of zebrafish heparan sulfate 6-*O*-sulfotransferase (*hs6st*). We demonstrate that Hs6st transfers sulfate specifically to position 6 of *N*-sulfoglucosamine. During early development, *hs6st* is expressed most prominently in the somites, the brain, and the fins. A loss-of-function phenotype obtained by injection of morpholino antisense oligonucleotides results in a significant and specific inhibition of 6-*O*-sulfation and affects structures that express *hs6st*. Importantly, morphants display disrupted somitic muscle development due to the combined effect of impaired anterior somite specification and later defects in muscle differentiation, which eventually leads to severe muscle degeneration.

EXPERIMENTAL PROCEDURES

Zebrafish and Embryos—Zebrafish (Danio rerio) were kept and bred according to standard protocols (16).

EST Clone, Chemicals, and Morpholinos—The zebrafish EST clone (RZPD CloneID MPMGp609N1048; accession no. fd09d05.y1) was purchased from the Deutsches Ressourcenzentrum für Genomforschung GmbH (RZPD). Heparitinase I (EC 4.2.2.8), II and III (EC 4.2.2.7), chondroitin, CDSNS-heparin, 6ODS-heparin, heparan sulfate from pig aorta, heparan sulfate from EHS tumor and an unsaturated heparan sulfate disaccharide kit were obtained from Seikagaku Corp. NS-heparosan was prepared by chemical deacetylation and *N*-sulfation from *N*-acetyl heparosan, which was prepared from *Escherichia coli* K5 by Dr. Terumi Saito, Kanagawa University. [^{35}S]PAPS was prepared as described previously (17). Standards of unsaturated disaccharides were purchased from Seikagaku Corp. Morpholinos were designed by and obtained from Gene Tools, LLC. Sequences were as follows: Hs6st-MO (1), 5′-GATTTCCCATCCATCTTCTCGCTGG-3′, Hs6st-MO (2), 5′-GTGAAAGCATTACTCGGTTGTGCGG-3′, inverted Hs6st-MO, 5′-GGTCGCTCTTCTACCTACCCTTTAG-3′. Morpholinos were solubilized in injection buffer (18) at the concentration of 50 mg/ml. The resulting stock solution was diluted to working concentrations as indicated, in injection buffer prior to injection into one to four-cell stage zebrafish embryos.

Genetic Mapping Analysis—Radiation hybrid mapping was carried out as described previously (19).

In Situ Hybridization—Probe synthesis and *in situ* hybridization were carried out as described previously (20).

Construction of pFLAG-CMV2-hs6st—For the construction of the expression vector, the PCR product containing the open reading frame of *hs6st* was inserted into the pFLAG-CMV2 expression vector (Eastman Kodak Co.).

Tranfection of cDNAs and Transient Expression of Hs6st in COS-7 Cells—COS-7 cells (5.5×10^5) precultured for 48 h in a 60-mm culture dish were transfected with 5 μg of pFLAG-CMV2-*hs6st* or pFLAG-CMV2 alone using LipofectAMINE according to the manufacturer's recommended protocol (TransFact, Promega). After incubation in Dulbecco's modified Eagle's medium containing 10% (v/v) fetal calf serum and antibiotics for 72 h, the cells were washed with PBS(−), scraped, and homogenized in 1 ml of 10 mM Tris-HCl, pH 7.2, 0.5% (w/v) Triton X-100, 0.15 M NaCl, 20% glycerol, 10 mM $MgCl_2$, and 2 mM $CaCl_2$. The homogenates were subjected to stirring for 1 h and then centrifuged at $10,000 \times g$ for 30 min. FLAG fusion proteins in the supernatant (cell extract) were isolated by anti-FLAG M2 (Sigma) affinity chromatography according to the manufacturer's protocol, and the activities of Hs6sts in the supernatants and FLAG-bound fractions were measured as described below.

Assay for Sulfotransferase Activities—Sulfotransferase activities were determined as described previously (23). Briefly, the standard reaction mixture (50 μl) contained 2.5 μmol of imidazole-HCl, pH 6.8, 3.75 μg of protamine chloride, 25 nmol (as hexosamine; 500 μM) of acceptor glycosaminoglycans, 50 pmol of [^{35}S]PAPS (about 5×10^5 cpm, 1 μM), and enzyme. After incubation for 20 min at 37 °C, the reaction was stopped by heating at 100 °C for 1 min. Carrier chondroitin sulfate A (0.1 μmol as glucuronic acid) was added to the reaction mixture and the ^{35}S-labeled polysaccharides were isolated by precipitation with ethanol containing 1.3% potassium acetate and 0.5 mM EDTA, followed by gel chromatography on a Fast Desalting column to remove [^{35}S]PAPS and its degradation products. The amounts of enzymes added to the reaction mixture were chosen so as to obtain a linear incorporation of [^{35}S]sulfate. One unit of enzyme activity was defined as the amount required to transfer 1 pmol of sulfate/min to CDSNS-heparin. Analysis of the reaction products for the specificity and sulfation position was performed by HPLC as described previously (23) with some modifications. Briefly, ^{35}S-labeled products were digested with a mixture of 10 milliunits of heparitinase I, 5 milliunits of heparitinase II, and 10 milliunits of heparitinase III in 40 μl of 50 mM Tris-HCl, pH 7.2, 1 mM $CaCl_2$, and 4 μg of bovine serum albumin at 37 °C for 2 h. The digests were subjected to gel chromatography on Superdex 30 pg equilibrated with 0.2 M NH_4HCO_3. The ^{35}S-labeled disaccharide fractions were injected into a PAMN column together with standard unsaturated disaccharides of the kit. Fractions of 0.6 ml were collected and radioactivity was measured.

Chromatographic Analysis of Isolated Glycosaminoglycans of Zebrafish Embryos—Embryos at the one-cell stage were injected with 1.0 ng of Hs6st-MO (1) and 1.5 ng Hs6st-MO (2) simultaneously. Embryos were collected at the 48 hpf stage and freeze-dried. The dried samples were treated with 0.2 M NaOH for 16 h at room temperature. Subsequently, samples were neutralized with 4 M HAc, DNase, and RNase were added and incubated for 2 h at 37 °C. Then proteinase K was added, and the reaction mixture was incubated for 16 h at 37 °C. The reaction was stopped by heating at 100 °C for 5 min, and samples were centrifuged at 13,000 rpm for 10 min to remove insoluble material. The supernatants were diluted with an equal volume of Tris-HCl buffer (50 mM, pH 7.2) and loaded on a DEAE-Sephacel column equilibrated with Tris-HCl buffer containing 0.2 M NaCl. The columns were washed with 10 column volumes of Tris-HCl buffer and then eluted with 4 column volumes of 2 M NaCl in Tris-HCl buffer. The eluates were precipitated with 2.5 volumes of cold 95% ethanol containing 1.3% potassium acetate and the glycosaminoglycans were recovered by centrifugation. The GAGs were digested with a mixture of 10 milliunits of heparitinase I, 5 milliunits of heparitinase II, and 10 milliunits of heparitinase III in 40 μl of Tris-HCl buffer, 1 mM $CaCl_2$ and 4 μl of bovine serum albumin at 37 °C for 2 h. After filtration of the digests with Ultrafree-MC, unsaturated disaccharides in the filtrates were analyzed by a reversed-phase ion-pair chromatography using Senshu Pak column Docosil and determined with a fluorescence detector.

Bodipy-ceramide Staining—Bodipy-ceramide labeling was performed as described (21).

RESULTS

Isolation of Zebrafish hs6st—To isolate genes that may participate in neural plate regionalization, a subtractive hybridization experiment was performed.[2] One of the resulting cDNA clones, R1, was sequenced and appeared to be a partial *hs6st* cDNA clone. We obtained the full-length clone by searching the zebrafish EST data base. One clone (MPMGp609N1048) was 100% identical to the cDNA fragment so we sequenced it to completion. The largest open reading frame encoded a protein of 469 amino acids (Fig. 1*A*), which was homologous to HS6STs from various organisms (Table I). Highest homology was found to the human and murine HS6ST-1 and HS6ST-2 proteins. However, by amino acid comparison (Table I) and phylogenetic tree analysis (Fig. 1*B*) we could not assign zebrafish Hs6st to

[2] R. J. Bink, J. Joore, S. van de Water, and D. Zivkovic, manuscript in preparation.

A

```
MDGKSNYSRLLIALLMILFFGGIVLQYICSTSDWQLLHLASLSSRLGSRA      50
PGDRLNGAGAGDPYSSEDGALVRFVPRFNFTTKDLSRAVDFHIKGDDVIV     100
FLHIQKTGGTTFGRHLVRNIQLERPCECHAGQKKCTCYRPGKRDTWLFSR     150
FSTGWSCGLHADWTELTNCVPSFMSNRESQERRMTPSRNYYYITILRDPV     200
WRYLSEWRHVQRGATWKASKHMCDGRLPTLTELPSCYPGDDWSGCSLEEF     250
MVCPYNLANNRQTRMLADLSLVGCYNLTVMSENQRWAMLLESAKRNLRNM     300
AFFGLTEYQRKTQYLFEHTFRLSFIAPFTQLNGTRAASVEVEPETQRRIR     350
ELNQWDVELYEYARDLFLQRFQFARQQERREARQRRIQERRKLRAKVKSW     400
LGVTGKAVFKPTKEPPMTEQSPAFAEEKQADAEQTLESETEGQVEENWLE     450
EDDGEIMLDYSENVEQWR.
```

B

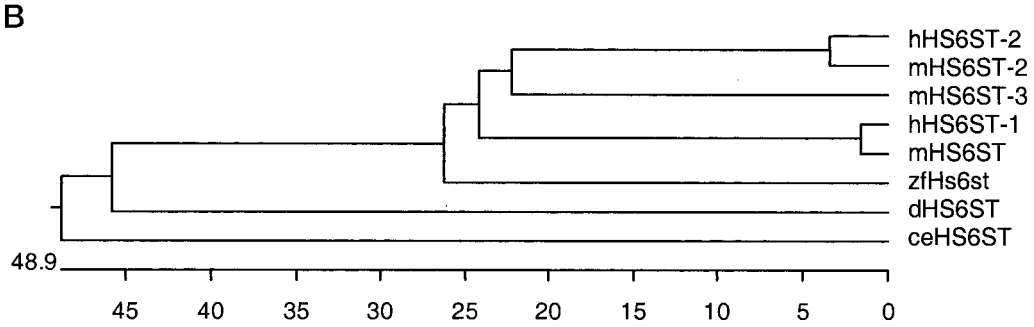

FIG. 1. **The deduced amino acid sequence and phylogenetic relationships of the Hs6st gene product.** *A*, the deduced amino acid sequence of the Hs6st gene product. In the protein sequence, the putative PAPS binding sites that were predicted by x-ray crystallography analysis of estrogen sulfotransferase (22) are underlined for 5′-phosphosulfate and for 3′-phosphate in PAPS. Two potential *N*-glycosylation sites are indicated (*bold italic*). DNA and amino acid sequences of Hs6st were submitted to GenBank™/EMBL (accession: AJ505990). *B*, phylogenetic tree of murine (*m*), human (*h*), zebrafish (*zf*), *Drosophila* (*d*), and *C. elegans* (*ce*) HS6ST proteins.

TABLE I
Amino acid sequence comparison of zebrafish Hs6st with HS6ST homologues of other species (23, 52, 53, 54, 81)

HS6STs	Identity
	%
Human HS6ST-1	56.9
Human HS6ST-2	55.9
Mouse HS6ST-1	56.1
Mouse HS6ST-2	55.2
Mouse HS6ST-3	51.8
Drosophila HS6ST	38.4
C. elegans HS6ST	37.6

TABLE II
Overexpression of zebrafish heparan sulfate 6-O-sulfotransferase in COS-7 cells

COS-7 cells were transfected with vector alone (FLAG-CMV2) or plasmid containing the zebrafish *hs6st* (FLAG-CMV2-*hs6st*). Enzyme activities of HS6ST and HS2ST in the cell extract were determined as described under "Experimental Procedures." Values represent means ± S.D. of triplicate independent experiments.

Plasmids	HS2ST activity	HS6ST activity
	pmol/min/mg protein	*pmol/min/mg protein*
FLAG-CMV2-*hs6st*	1.6 ± 0.1	4.2 ± 0.1
FLAG-CMV2 (control)	1.5 ± 0.1	1.3 ± 0.1

TABLE III
Acceptor substrate specificities of the recombinant zebrafish heparan sulfate 6-O-sulfotransferase purified by anti-FLAG antibody affinity column chromatography

Sulfotransferase activities were assayed using various glycosaminoglycans as acceptors and the values indicate the rate of incorporation into various substrates relative to that into CDSNS-heparin. Sulfotransferase fractions were prepared from COS-7 cells transfected with pFLAG-CMV-*hs6st*.

Substrate	Relative sulfotransferase activity of Hs6st
	%
CDSNS-heparin	100
CDSNAc-heparin	2.6
NS-heparosan	9.1
Heparan sulfate (mouse EHS tumor)	27.4
Heparan sulfate (pig aorta)	10.9
6ODS-heparin	2.1
Chondroitin	0

one of the two homologues. By calculating a Kyte-Doolittle hydrophobicity plot of the Hs6st protein sequence, a hydrophobic segment was found in the amino-terminal part (data not shown) that is characteristic for heparan sulfotransferases (23). This hydrophobic segment suggests that Hs6st is a type II transmembrane protein located in the Golgi apparatus where HSPGs are synthesized initially (24).

The genetic map position of *hs6st* was determined by radiation hybrid mapping (19). *hs6st* colocalizes with z3872 mapped on linkage group 14 (55.5 cM from top) of the MGH zebrafish map (zebrafish.mgh.harvard.edu).

Determination of Heparan Sulfate 6-O-Sulfotransferase Activity—The *hs6st* cDNA was transfected into cultured cells, and the expressed protein was examined for the HS6ST activity. The HS6ST activity, defined as the amount required to transfer 1 pmol of sulfate/minute to CDSNS-heparin, in cells transfected with *hs6st* was more than 3-fold higher as compared with the control vector (Table II). The HS2ST activity was not changed upon transfection of *hs6st*. These results demonstrate that recombinant Hs6st transfers sulfate to position 6 of *N*-sulfoglucosamine residues in CDSNS-heparin.

To compare the sulfotransferase activity of zebrafish Hs6st to that of other organisms, we investigated its sulfotransferase activity for various heparin derivatives, heparan sulfates from different sources, and other GAGs (Table III) including: CDSNS-heparin, CDSNAc-heparin, NS-heparosan, heparan sulfate from mouse EHS tumor and pig aorta, 6ODS-heparin, and chondroitin. Hs6st was able to transfer sulfate to CDSNS-heparin, NS-heparosan, and heparan sulfate but not to CDSNAc-heparin, 6ODS-heparin, and chondroitin. Furthermore, the ratio of the activity between NS-heparosan and CDSNS-heparin was less than 0.1 at all the concentrations tested

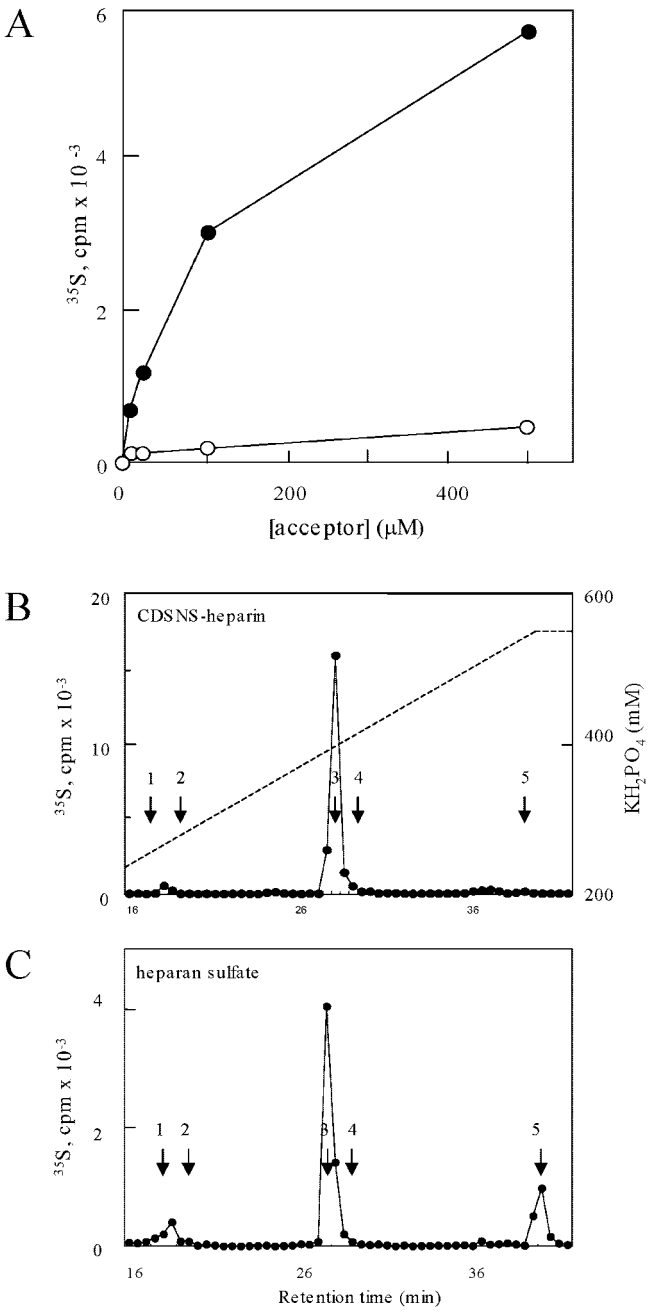

FIG. 2. **Analysis of Hs6st activity and acceptor substrates.** *A*, effects on the activities of Hs6st of variable concentrations of acceptor substrates. The activities of sulfotransferases were measured using 0.07 units of the recombinant enzymes as described under "Experimental Procedures" except that various amounts of CDSNS-heparin (●) or NS-heparosan (○) were added. Values represent means of duplicate independent experiments. *B* and *C*, HPLC analysis of ^{35}S-labeled products derived from CDSNS-heparin (*B*) and heparan sulfate of pig aorta (*C*) incubated with purified recombinant Hs6st and [^{35}S]PAPS. Labeled products by sulfotransferase reactions were digested with a mixture of heparitinases and the disaccharide fractions were subjected to PAMN columns. The *dotted line* in *B* indicates the concentrations of KH_2PO_4 for the elution. The *black dots* (●) show the elution patterns of ^{35}S-labeled digests. The *arrows* in *B* and *C* indicate the elution positions of: ΔDi-6S (1), ΔDi-NS (2), ΔDi-(N,6)diS (3), ΔDi-(N,2)diS (4), ΔDi-(N,6,2)triS (5).

(Table III, Fig. 2*A*). This indicates that Hs6st preferred iduronosyl *N*-sulfoglucosamine since NS-heparosan contains only glucuronic acid and not its epimer iduronic acid. These data are very similar to the sulfotransferase activity values found for mHS6ST-1 and not to values for mHS6ST-2 (23).

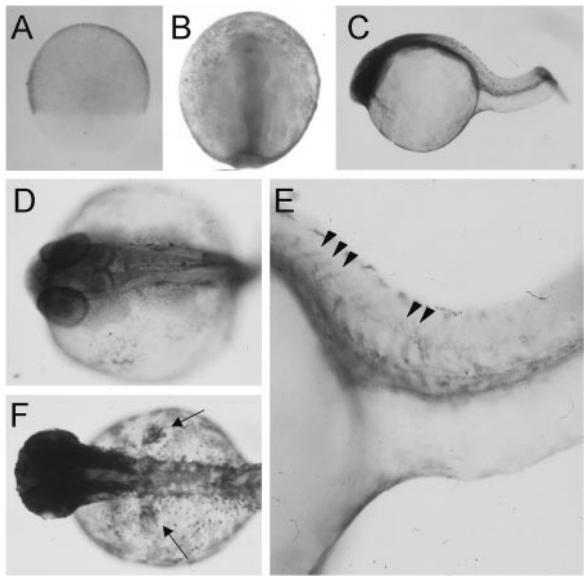

FIG. 3. ***In situ* expression pattern of *hs6st* mRNA.** *A*, ubiquitous expression at the 60% epiboly stage. *B*, a seemingly concentrating expression to the prospective brain at the 2-somite stage, dorsal view, anterior up. *C*, expression of *hs6st* in the brain and the anterior trunk at 24 hpf, lateral view, anterior to the left. *D*, expression in the head at 24 hpf in a dorsal view. *E*, expression in the somite boundaries (*arrowheads*) and in the ventral part of the posterior trunk at 24 hpf. *F*, expression at 48 hpf showing *hs6st* transcripts in the head and in the finbuds (*arrows*), dorsal view.

To further determine the specificity of Hs6st function, the structure of the ^{35}S-labeled products was analyzed after incubation of purified Hs6st, ^{35}S-labeled PAPS and CDSNS-heparin or heparan sulfate of pig aorta (Fig. 2, *B* and *C*). Most of the radioactivity in the disaccharide fractions derived from both acceptor substrates was recovered at the position of ΔDi-(*N*,6)diS, and a low level of radioactivity eluted in an unknown peak between ΔDi-6S and ΔDi-NS. Furthermore, ^{35}S-labeled ΔDi-(*N*,6,2)triS was also produced using heparan sulfate as acceptor. These results show that Hs6st transfers sulfate groups to position 6 of GlcNSO3 residues and to position 6 of $GlcNSO_3(6SO_4)$ residues.

Expression Pattern of hs6st during Zebrafish Embryonic Development—Northern blot analysis revealed that *hs6st* was not maternally expressed (data not shown). The spatio-temporal pattern of zygotic *hs6st* expression was analyzed by whole mount *in situ* hybridization. At the onset of gastrulation, *hs6st* is ubiquitiously expressed in the entire blastoderm (Fig. 3*A*). During early somitogenesis the staining seems to concentrate to the anterior CNS (Fig. 3*B*). Consistently, at 24 hpf the brain and the eyes of the embryo show intense staining. Importantly, expression was also restricted to the somitic boundaries as well as to the ventral part of the tail (Fig. 3, *C–E*). The rostral expression persisted until at least the 48 hpf stage when the fin buds contained high levels of the *hs6st* transcripts as well (Fig. 3*F*).

Morpholino-mediated Knockdown of Hs6st Results in Specific 6-O-Sulfation Inhibition—To assess the developmental function of Hs6st, we have selectively blocked the translation of the *hs6st* mRNA using morpholino antisense oligonucleotides, which have been proven to be effective and specific translational inhibitors in zebrafish (18) and were shown to phenocopy a wide variety of earlier described mutations (25). For knockdown experiments we used two morpholinos of non-overlapping sequence as this method yielded a higher frequency of knockdown phenotypes whereas possible nonspecific undesired mistargeting effects were reduced (Ref. 26, data not shown).

TABLE IV
Disaccharide composition analysis in wild-type and Hs6st morphants

Hs6st morpholino injection results in specific 6-*O*-sulfation decrease as judged from the HPLC analysis of disaccharide components of 48 hpf wild-type and morphant samples. Second and third columns; absolute HPLC values for different residues: fourth column, relative increase and decrease of disaccharide composition.

	Wild type	Morpholino injected	Relative in/decrease
			%
Di-OS	53.0	57.3	+8.1
Di-NS	15.4	17.2	+11.7
Di-6S	5.5	4.4	−20.0
Di-(N,6)diS	6.2	3.7	−40.3
Di-(N,U)diS	9.7	8.7	−10.3
Di-(N,6,U)triS	10.2	8.8	−13.7

This technique allowed us to specifically inhibit 6-*O*-sulfation, which is a great advantage when compared with the more general inhibition of proteoglycan/protein sulfation by for example chlorate (27–29). As controls, inverted morpholinos were used (see "Experimental Procedures") that resulted in wild-type embryos upon injection.

Specificity of the injected morpholinos was assessed by determining the sulfation profile of disaccharide components of wild-type *versus* morpholino-injected embryos that showed the morphant phenotype. In 48 hpf embryos, highest decrease of sulfation (40.3%) in morphants was found for 6-*O*-sulfation of *N*-sulfoglucosamine residues (production of ΔDi(N, 6)diS (Table IV)). As compared with the disaccharide components of wild-type embryos, *N*-sulfation increased, and 2-*O*-sulfation decreased slightly (Table IV). Analysis of heparan sulfate compositions was performed in duplicate with a similar outcome. From these results, we conclude that Hs6st morpholino injection inhibits 6-*O*-sulfation specifically albeit not completely.

Phenotypic Characteristics of Hs6st Morphants—The morpholino-mediated knockdown of Hs6st activity resulted in dramatic phenotypic abnormalities that were already visible during somitogenesis (Fig. 4). Control experiments in which embryos were injected with inverted Hs6st-morpholinos did not alter the wild-type phenotype throughout development indicating the specificity of the morpholinos (Fig. 4, *A* and *B*). Embryos injected with Hs6st morpholinos demonstrated convergent-extension defects, reminiscent of *knypek* (*kny*)/*glypican* zebrafish mutants (7), that became more obvious as development proceeded (Fig. 4*C*, see also Fig. 6, *G–J*). Often the tail was curled and to a certain extent, morphants displayed transient and variable brain apoptosis between 24 and 48 hpf (Fig. 4*C*). As a consequence, the size of the head in morphants was reduced later in development (Fig. 4, *D* and *E*). In contrast, the brain ventricles had an inflated and oedemic appearance possibly due to the overproduction of cerebrospinal fluid. Transverse sections of the brain of 48 hpf embryos show that both the size of the white matter composed of the nerve tracts and the gray matter composed of somata, were significantly reduced in Hs6st morphants although the gray matter was relatively less affected (Fig. 4, *F* and *G*). Strikingly, we also regularly observed a reduction in the size of the pectoral fins at 96 hpf (Fig. 4, *D* and *E*), a structure that showed expression of *hs6st* (Fig. 3*F*).

Knockdown of Hs6st Disrupts Muscle Development in Zebrafish—The most obvious defects in Hs6st knockdown embryos were seen in somite development. Nomarski images of somites of 48 hpf morphant embryos reveal abnormal muscle fiber structure with undifferentiated cells present (Fig. 5, *A–C*). To investigate somite abnormalities further, we utilized Bodipy-ceramide, a lipophilic, vital dye to reveal cell morphology. In 24 hpf wild-type embryos, somites have a chevron shape with clear boundaries. The adaxial cells at the horizontal myoseptum can be clearly distinguished by their morphology (Fig. 5*D*). Morpholino injections resulted in a range of phenotypes that could qualitatively be categorized as weak, intermediate, or strong. In weakly affected Hs6st morphants, muscle cell morphology is normal but there are local interruptions in the vertical myoseptae, which result in cells spanning across the somitic boundary (Fig. 5*E*). In embryos with qualitatively more severe defects, however, muscle differentiation seems to be affected at an earlier step. Some somitic cells are smaller, do not show the classic elongated shape observed in wild-type embryos and breakdown of intersomitic boundaries is even more pronounced (Fig. 5*F*). By 72 hpf, somite defects become very severe in morphant embryos (Fig. 5, *G–I*). In less strongly affected embryos, somites have large rounded cells, which appear to be only empty shells with intact membrane surrounding them as shown by their exclusion of Bodipy-ceramide (Fig. 5*H*). In more severe cases, muscle degeneration is almost complete, the empty cells observed in weaker affected embryos are completely reabsorbed leaving large intercellular spaces with barely a few muscle cells remaining connected to each other and to the remnants of the intersomitic boundaries (Fig. 5*I*). The fact that we observed slight qualitative differences in severity of morphant phenotypes within the same batches of injection experiments as indicated by weak (Fig. 5, *B*, *E*, *H*) and strong (Fig. 5, *C*, *F*, *I*) phenotypes may be due to unequal spreading of injected morpholino solution resulting in slightly different active concentrations in the early embryo. This could

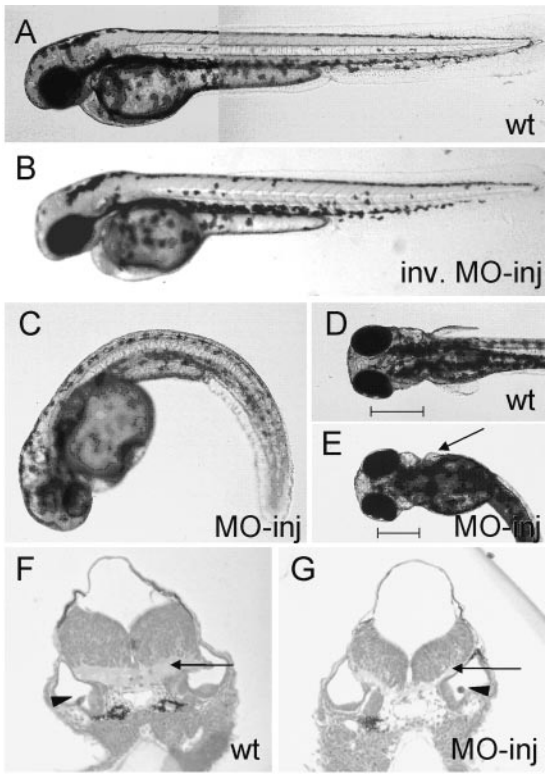

FIG. 4. **Phenotypical defects of Hs6st morphants.** *A*, lateral view of a 48 hpf wild-type embryo. *B*, lateral view of a 48 hpf embryo injected with 3.75 ng Hs6st inverted morpholino. *C*, lateral view of a 48 hpf Hs6st morphant of reduced size displaying a curly tail. *D* and *E*, dorsal view of a 96 hpf wild-type embryo (*D*) and a 96 hpf morphant (*E*). The size of the mid- and hindbrain as can be seen by the distance from the middle of the lens to the posterior end of the ear (*bar*) as well as the size of the fin (*arrow*) was reduced. *F* and *G*, transversal sections of 48 hpf embryos at the level of the otic vesicle (*arrowhead*) show a strong reduction of the white matter (*arrow*) in a representative morphant (*G*) as compared with the wild-type (*F*). Injections were done with 1.0 ng of Hs6st-MO (1) and 1.5 ng of Hs6st-MO (2). *Wt*, wild type; *inv. MO-inj.*, inverted Hs6st morpholino-injected; *MO-inj.*, Hs6st morpholino-injected.

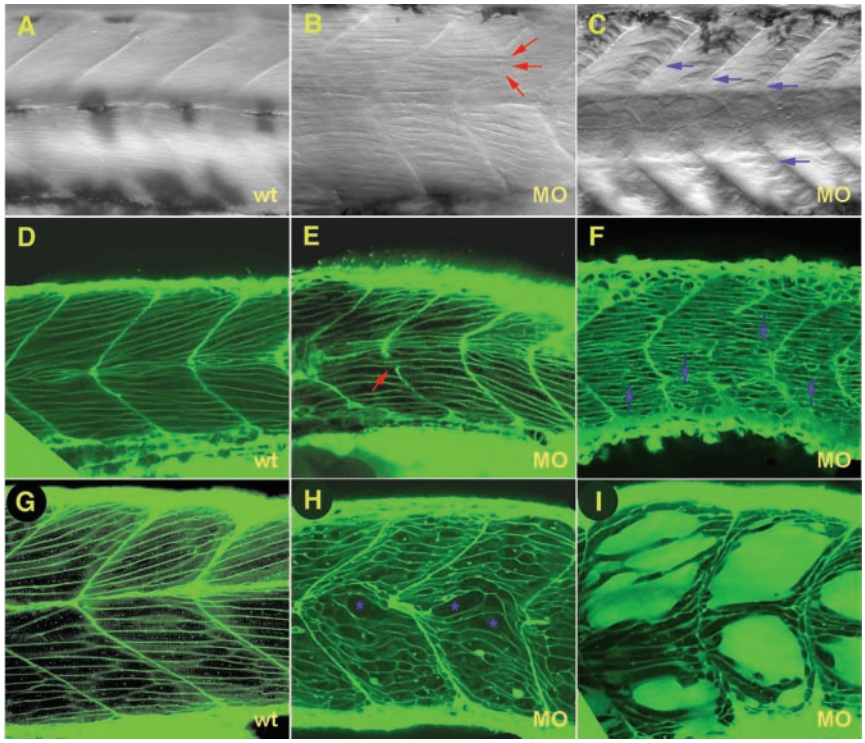

FIG. 5. **Somitic muscle degeneration in Hs6st morphants with phenotypes qualitatively categorized as weak or strong.** Lateral views of wild-type (*A*, *D*, *G*), weaker (*B*, *E*, *H*), and stronger (*C*, *F*, *I*) morphant somite phenotypes as revealed by DIC microscopy and by Bodipy-ceramide staining and confocal microscopy. *Red arrows* show breakdown of somitic boundaries, *blue arrows* indicate small, round, undifferentiated-looking cells. *Blue asterisks* show the large empty cells surrounded by intact cell membrane. *A–C*, 48 hpf; *D--F*, 24 hpf; *G–I*, 72 hpf. *Wt*, wild type; *MO*, morpholino-injected.

result in mild and strong phenotypes at later stages of development.

Knockdown of Hs6st Does Not Affect the Somite Oscillator Mechanism but Disturbs Expression of Anterior Somite Markers—Next we set out to investigate what mechanism leads to the abnormal somitic boundaries observed in morphant embryos. To this end expression of different marker genes was assessed in qualitative terms. In 10-somite stage wild-type embryos *myoD*, a bHLH transcription factor involved in muscle differentiation is expressed in adaxial cells and in the posterior part of the newly formed somites (Refs. 30 and 31, Fig. 6*A*). In 15-somite stage Hs6st morphants the striped pattern in the mature somites is severely disturbed (Fig. 6*B*). We hypothesized that the oscillator mechanism regulating zebrafish somitogenesis might be affected. To this end, we analyzed the expression pattern of *her1* and *deltaD*, two effectors of the zebrafish somitic clock (32, 33, 34). In embryos with perturbed oscillator function, *her1* and *deltaD* are expressed throughout the presomitic mesoderm instead of the normal stripe pattern (35). Even severe Hs6st morphants, however, displayed a wild-type-like *her1* and *deltaD* stripes of expression in the most recent forming somites (Fig. 6, *C–F*) suggesting that the oscillator function is not affected by Hs6st knockdown. Interestingly however, the striped pattern shows left-right asymmetry in about one-third of the injected embryos, which suggests asynchrony during somite development.

To examine antero-posterior specification within the somites, *notch5* and *notch6*, two genes encoding Delta receptors and expressed in the posterior and anterior part of the somites, respectively, were analyzed (36). At the 10-somite stage, somites were expanded laterally as judged from *notch5* and *notch6* expression patterns most likely due to early aberrant convergent extension movements (Fig. 6, *G–J*). In contrast to the defects observed with later *myoD* distribution, Hs6st morphants did not display obvious change in the expression pattern of *notch5* indicating that posterior somite identity was unaffected (Fig. 6, *G* and *H*). Expression of *notch6* in the last 4–5 somites however was somewhat reduced, which suggests that anterior somite specification may be impaired (Fig. 6, *I* and *J*). *Mesp-b* is a functional homologue of mammalian *mesp2* (37), a bHLH transcription factor, which is segmentally expressed in two or three stripes in the anterior regions of somite primordia and is responsible for anterior somite specification upstream of *notch5* and *notch6* in zebrafish (Refs. 38 and 39, Fig. 6*K*). Knockdown of Hs6st results in reduced expression of *mesp-b* at the 5-somite stage as compared with wild-type expression but the segmental pattern of the transcript is still detectable (Fig. 6, *K* and *L*). These results suggest that partial loss-of-function of Hs6st does not impair the somitic clock mechanism but affects later *mesp-b*-dependent steps during somite patterning.

Hs6st Is Required for Proper Muscle Differentiation—To investigate the molecular basis of somitic defects we analyzed marker genes involved in muscle development. In 24 hpf wild-type embryos, *myoD* is expressed in the individual somites in which expression of *myoD* in the posterior-most somites is slightly stronger (Fig. 7*A*). In morphant embryos, *myoD* is clearly expressed more intensely in all somites along the antero-posterior axis (Fig. 7*B*). As development proceeds, *myoD* is down-regulated in wild-type embryos with only remnants of *myoD* mRNA left in the somites (Fig. 7, *C* and *E*). Interestingly, *myoD* expression is maintained at high level in the somites of 48 hpf morphant embryos (Fig. 7, *D* and *F*) suggesting that differentiation is perturbed. As it is possible that lingering activity of *myoD* interferes with the process of normal differentiation, we next examined *α-tropomyosin* expression, one of the first structural protein genes to be activated during this process (40). However, no changes were detected in its expression indicating that the initial steps of differentiation proceeded correctly (Fig. 7, *G* and *H*). Slow muscle in zebrafish develops from a subset of somitic cells, which can be found closest to the notochord and therefore referred to as adaxial cells (41, 42). Muscle pioneer (MP) cells differentiate from the adaxial cells and express *eng2* (43, 44). As early *myoD* expression indicated that adaxial cell specification is normal, we examined whether separation of MP cells from the adaxial cell lineage occurred properly. We found that *eng2* mRNA levels were significantly higher along the A-P axis but no lateral or

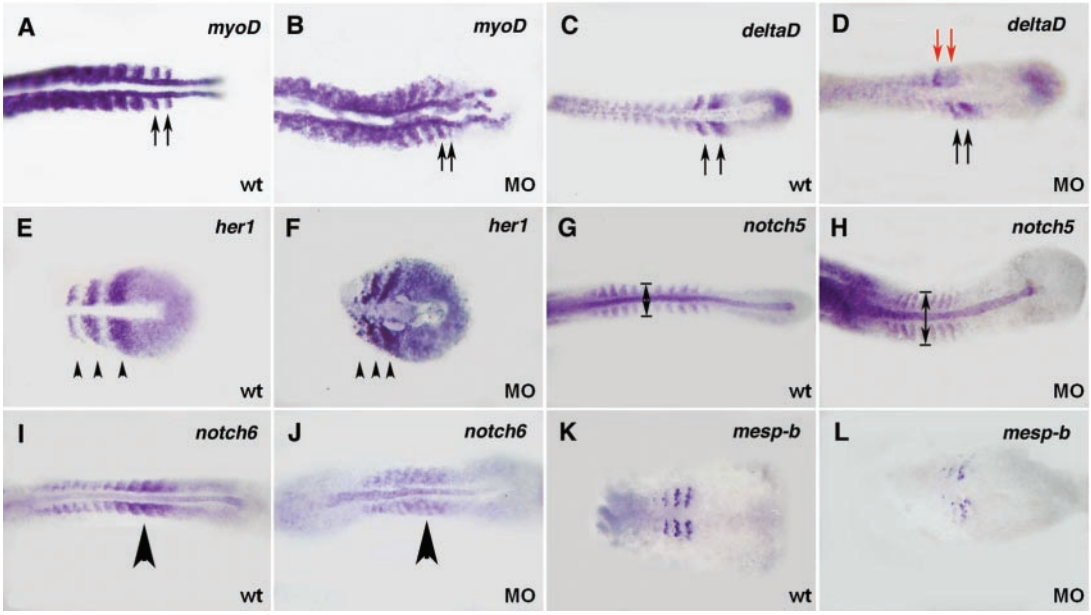

FIG. 6. **Hs6st morphants display normal somite oscillator function but have impaired anterior somite specification as shown by qualitative analysis of expression of marker genes.** *A* and *B*, expression of *myoD* in the mature somites is disrupted in morphants. *C–F*, expression of *deltaD* (*C* and *D*) and *her1* (*E* and *F*) is comparable in wild-type and Hs6st morphants. *G* and *H*, expression of *notch5* in the posterior half of the somites is normal in Hs6st morphants as compared with wild type. *I* and *J*, expression of *notch6* in the anterior half of the somites is reduced particularly in the posteriormost somites of Hs6st morphants. *K* and *L*, expression of *mesp-b* in the forming somites is reduced but still present in Hs6st morphants. *A* and *B*, 15-somite stage; *C* and *D*, *G–J*, 10-somite stage; *E*, *F*, *K*, *L*, 5-somite stage. *Small black arrows* and *arrowheads* indicate the striped expression pattern of various genes. The *red arrows* show left-right asymmetry in *deltaD* expression. *Large black arrowheads* in *I* and *J* show decreased *notch6* expression in morphant embryos. *Double arrows* in *G* and *H* indicate the increased width of morphant embryos as compared with wild type. *Wt*, wild type; *MO*, morpholino-injected.

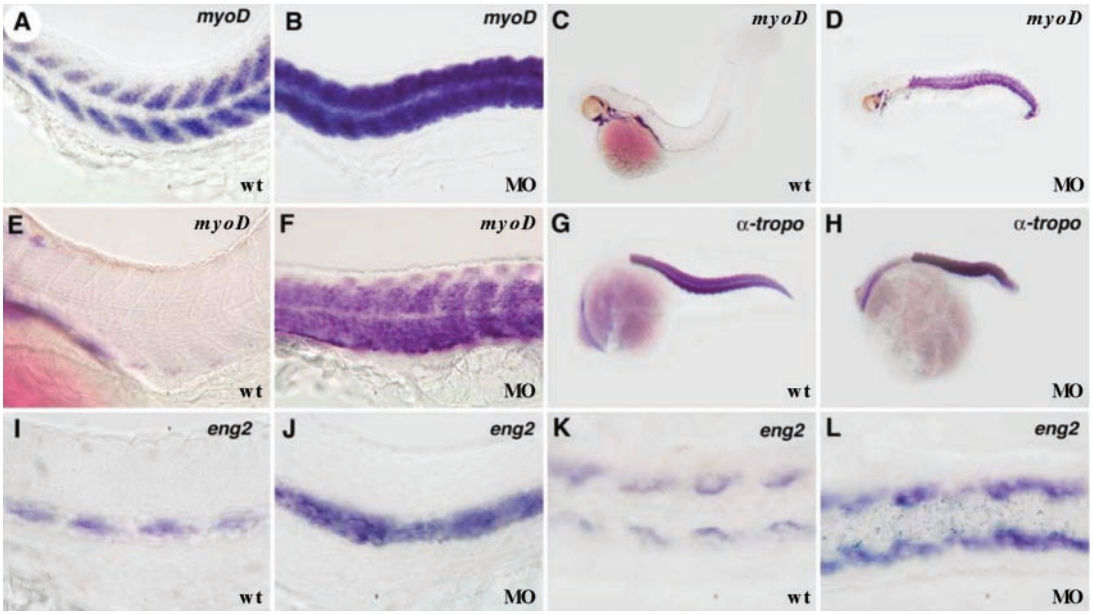

FIG. 7. **Muscle differentiation is perturbed in Hs6st knockdown embryos.** *A* and *B*, elevated expression of *myoD* in the horizontal midline and in the anterior part of the somites of 24 hpf morphants. *C–F*, *myoD* expression remains high in 48 hpf morphant embryos. *G–H*, expression of *α-tropomyosin,* one of the first terminal differentiation markers in the somites, is not affected in 24 hpf morphants. *I–L*, expression of *eng2* along the A-P axis is enhanced at 24 hpf in Hs6st morphants. *Wt*, wild type; *MO*, morpholino-injected.

dorsoventral expansion was detected (Fig. 7, *I–L*). These results suggest that somitic muscle differentiation is arrested at an early stage, which might lead to its later degeneration.

As signals from axial tissues are known to regulate gene expression in paraxial mesoderm, we next investigated structural integrity and signaling from the axial mesoderm. In zebrafish, the gene coding for the α chain of type II collagen (*col2a1*), is expressed in a number of chondrogenic and nonchondrogenic tissues including the floorplate, the notochord and the hypochord (Refs. 45 and 46, Fig. 8*A*). In 24 hpf morphants, expression is present in all three tissues but mRNA levels remained elevated in the notochord whereas floorplate and hypochord expression decreased (Fig. 8*B*). Also, the cellular morphology of the vacuolar cells in the notochord is affected, which indicates that cellular proliferation or differentiation might be perturbed by Hs6st morphants.

Shh and other members of the Hedgehog family have been shown to regulate somite differentiation in zebrafish as well as

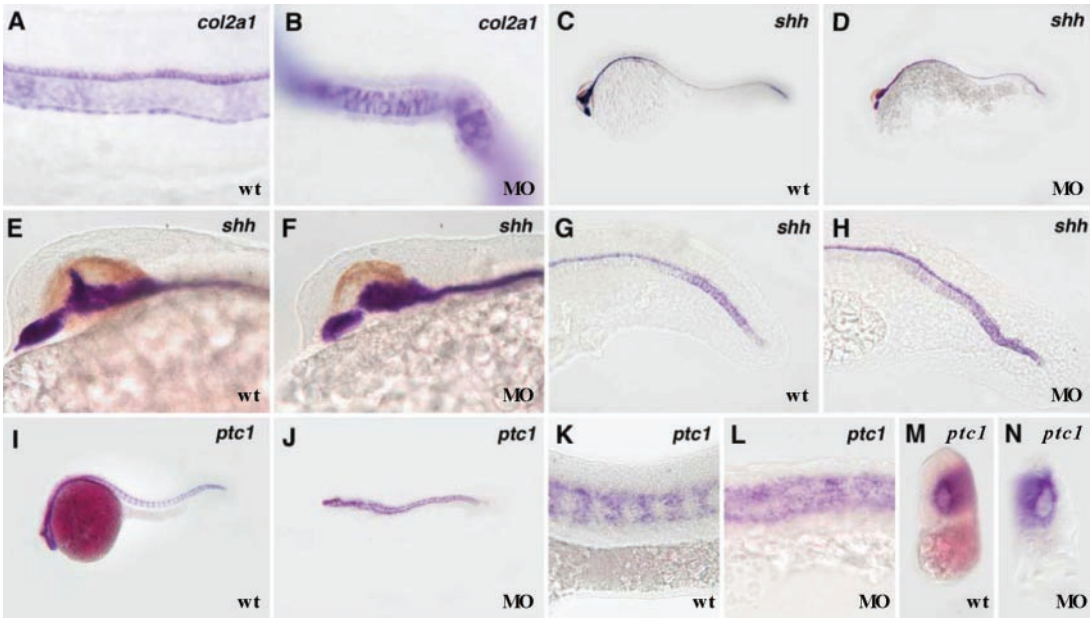

FIG. 8. **Expression pattern analysis of *col2a1*, *shh,* and *ptc1* in Hs6st morphants at 24 hpf.** *A* and *B*, lateral view of *col2a1* expression in a wild-type and in a Hs6st morphant embryo reveals the presence of midline axial mesodermic structures (notochord, hypochord) and an intact floor plate. *C–H*, normal expression of *shh* in the floorplate of Hs6st morphants. *E* and *F*, expression of *shh* in the head region. Hs6st morphants lack the dorsal expression at the zona limitans interthalamica found in wild-type embryos. *I–N*, somitic *ptc1* expression surrounding the notochord is normal in morphants. *A–L*, lateral views; *M* and *N*, optical cross-sections of the trunk. *Wt*, wild type; *MO*, morpholino-injected.

in higher vertebrates (47–49). In 24 hpf zebrafish embryos, *shh* is expressed in the brain, the floorplate and in the posterior end of the notochord (Ref. 50, Fig. 8, *C*, *D*, *G*, *H*). In 24 hpf morphants, notochordal, and floor plate expression was normal, but the dorsal extension of the zona limitans interthalamica, was absent (Fig. 8, *E* and *F*). To investigate if Hedgehog signaling from axial tissues is normal in morphant embryos we used the *patched1* (*ptc1*) marker gene. *Ptc1* is a *shh* receptor, expressed in a pattern complementary to that of *shh* in the central nervous system and in the paraxial mesoderm of zebrafish embryos and has been shown to be regulated by Hedgehog signaling (51). In Hs6st morphants, somitic *ptc1* expression surrounding the notochord is not affected indicating that enhancement of *eng2* expression is unlikely to be a result of altered Hedgehog signaling by Hs6st (Fig. 8, *I–N*).

In summary, the above *in vivo* experiments have shown that Hs6st is essential during somite specification and differentiation of muscle cells albeit Hs6st acts independent of the somite oscillator mechanism.

DISCUSSION

Enzymes that modify HSPGs play essential roles during development. The fact that an enormous structural diversity of GAGs is created by deacetylation, sulfation, and epimerization indicates that a complex scaffold of proteoglycans is attached to the cells. Heparan sulfate 6-*O*-sulfotransferase is one of these modifying enzymes and here we describe its expression, biochemical activity, and examine its functions during zebrafish muscle development.

In contrast to the mouse and human that have multiple HS6ST homologues (23, 52, 53), *Xenopus*, *Drosophila* and zebrafish have only one described gene coding for HS6ST so far (Refs. 6 and 54, this study). The 3-fold increase in HS6ST activity as found for zebrafish Hs6st was comparable to the values found in *Drosophila* for HS6ST activity (54). The phylogenetic analysis using simple homology search does not indicate clearly which is the true mouse orthologue of zebrafish *hs6st*. Comparison of expression data is not very informative in this regard as the study describing the expression patterns of putative homologues in mouse and *Xenopus* have been limited to later stages of development (6, 23). Biochemical evidence however, demonstrates that based on the ratio of HS6ST activity between CDSNS-heparin and NS-heparin (23), the zebrafish gene is acting in a fashion most similar to murine HS6ST-1. In biological assays to examine its cellular function we observed a specific HS6ST activity as sulfate groups were predominantly transferred to position 6 of *N*-sulfoglucosamine. Surprisingly, injection of two non-overlapping morpholinos did not result in a 100% inhibition of sulfate transfer as assessed by the analysis of disaccharide components in 48 hpf morphant and wild-type embryos. Unfortunately, due to the lack of an antibody against Hs6st, we were not able to analyze whether morpholino injection abolished Hs6st protein levels completely in morphant embryos, which leaves two possible explanations for the observed specific but partial 6-*O*-sulfation in morphants. Zebrafish may possess more than one gene coding for an enzyme with HS6ST activity similarly to the situation in the mouse and in humans (52, 53). Alternatively Hs6st activity may partially be recovered by 48 hpf of development, similarly to what was found for other proteins in transient knockdown studies (55–57).

In summary, our data suggest that zebrafish Hs6st is the homologue of mHS6ST-1. Whether zebrafish encodes multiple homologues of Hs6st can only be answered definitively upon completion of the zebrafish genome sequence.

The expression pattern of *hs6st* suggested a role in several developmental processes, which were confirmed in the functional knockdown experiments. *Hs6st* mRNA is present in three main areas in the zebrafish: the brain, the pectoral fins, and the somites. One characteristic of Hs6st morphants was the reduction of white matter in which axon bundles reside. HSPGs are highly abundant in the white matter of rat and chick embryonic brains and are involved in neurite outgrowth and axonal guidance (58, 59). Moreover, it has been shown that the composition of heparan sulfate with respect to 2-*O* and 6-*O* sulfation might be responsible for proper targeting of retinal ganglion cell axons in *Xenopus* (6). It is possible that in ze-

brafish other proteoglycans are involved primarily in this process as in our knockdown experiments optic nerve formation and the optic tract is not affected (data not shown). Supporting this idea is the recent data demonstrating that strong repellent guidance of regenerating optic axons in zebrafish embryos has mainly been ascribed to chondroitin sulfates but not to heparan sulfates (60). *Hs6st* expression was also found in the pectoral fins of 48 hpf zebrafish embryos. In accordance, morphant embryos display reduced pectoral fins at 5 dpf. The mechanism of Hs6st action in fin development is at present unclear and requires further study.

In vertebrates, almost all skeletal muscle is derived from the somites. Knockdown of Hs6st function appears to affect muscle development at several levels including: 1) perturbing *mespb*-dependent somite patterning demonstrating the impaired anterior somite specification, 2) maintaining high levels of *myoD* expression during somitogenesis in contrast to wild-type embryos that display a down-regulation of *myoD* expression as development proceeds indicating that differentiation processes are affected in Hs6st morphants, 3) causing severe muscle degeneration at later stages as observed by Bodipy-ceramide labeling, and *myoD* expression by an as yet unclear mechanism.

The zebrafish somitic clock, responsible for directing proper division of the unsegmented paraxial mesoderm, consists of *her1* and components of the Delta-Notch signaling pathway although the exact details of its mechanism are still under dispute (35, 61, 62). Expression of *notch6* that is localized to the anterior part of the somites is slightly reduced in Hs6st morphant embryos, particularly in the posteriormost, newly formed somites while expression of the posterior marker *notch5* is unaffected. *Mesp-b,* a gene involved in promoting anterior somite fate (38) was also perturbed in morphants suggesting that zebrafish Hs6st is required in a step of the A-P patterning pathway upstream of *mesp-b*. As the striped expression pattern of both *her1* and *deltaD* is present in Hs6st morphants, the observed *mespb*-dependent defects seem to occur without the direct involvement of the somite oscillator mechanism. These findings are in agreement with *her1* being active during anterior somite specification independently of *mesp-b* (38).

For proper differentiation of muscle precursor cells in the somites, the correct spatio-temporal activation of myogenic genes is required and these genes are regulated by Wnts, Hhs BMPs, and FGFs (63, 64) secreted by cells of various surrounding tissues. Recently, it has been demonstrated that expression of *myogenin* in the mouse limb bud (65), is temporally and spatially coincident with expression of two proteoglycan core protein genes, decorin, and syndecan-3 (66). Furthermore, syndecan-3 is synthesized by myoblasts and inhibition of its expression results in acceleration of muscle differentiation in an FGF-2-dependent manner (67). In Hs6st morphant zebrafish embryos, *myoD* expression in the somites is maintainted and increased as compared with wild-type embyros suggesting that proper sulfation might play a role in controlling proper spatio-temporal pattern of muscle differentiation. This is supported by the fact that we also observed an increase of *eng2* expression, a homeodomain repressor gene that is expressed in muscle pioneer cells along the somitic myoseptum (41). At later stages, we observed severe degeneration of muscle cells in the somites of Hs6st morphants indicating that the activity of Hs6st is essential for proper muscle cell development. Whether this feature is a direct consequence of the perturbed differentiation is currently unclear but our observation that *myoD* expression is not reduced in morphant somites might indicate a connection between these events. As *eng2* expression marks a subset of slow muscle forming adaxial cells in zebrafish that are not affected by knockdown of *hs6st*, further experiments are necessary.

HSPGs have a significant role in modifying various cellular signaling processes (2). One of the pathways, that has been shown in this context, is the Wnt pathway. Wnts have been shown to control myogenesis in mammalian systems (68, 69, 70). Wnts bind with high affinity to heparin and heparan sulfate and it is now generally thought that Wnt signaling is regulated through their binding to heparan sulfate moieties on cell surface HSPGs in the extracellular matrix (13, 71–75). Our data supports a genetic interaction between Hs6st and Wnt signaling as in Hs6st morphants we observed an up-regulation of *myoD* and *eng2* expression, which are both described as Wnt target genes in mice (76, 77). Also, the strong Hs6st knockdown phenotype is reminiscent to *kny*, a glypican mutant, which has severe convergent extension defects, that potentiates Wnt11 function in a dose-dependent manner (7). However, further experiments are needed to address the precise functional link between Hs6st and Wnt signaling in myogenesis.

Hedgehog signaling has also been linked to HSPG synthesis and sulfation. *Tout-velu*, a heparan-sulfate copolymerase gene related to the mammalian tumor supressor genes *EXT1* and *EXT2*, is required for proper diffusion of the long-range Hedgehog signal during wing disc patterning in *Drosophila* (10, 12). Mutants of the *sulfateless* gene have impaired *N*-deacetylase/*N*-sulfotransferase function and lack *N*-, 2-*O*-, and 6-*O*-sulfation. The *sulfateless* gene is essential for proper Wg, FGF as well as Hh signaling in *Drosophila* (9, 78, 79). Our experiments have revealed an increase in *eng2* expression in the somites; a feature that has been obtained previously by increased Hedgehog signaling (47). In contrast to our results however, these experiments also resulted in D-V as well as lateral expansion of *eng2*-expressing cells in the somites. Since this is not the case in Hs6st morphants it appears that Hs6st might not act by affecting midline Hedgehog signaling. This was confirmed by the unchanged expression of *ptc1*, a known Hh target gene (51).

In conclusion, this is the first report that demonstrates that reduced transfer of 6-*O*-sulfation by Hs6st to GAG chains causes developmental defects as shown in an *in vivo* situation during vertebrate development. Gross HSPG modifications are brought about by chemical compounds such as chlorate, a very potent, but nonspecific inhibitor of sulfation that reduces the PAPS concentration (27–29) and these modifications interfere with developmental processes such as neural tube closure (80). Our results demonstrate that even subtle changes in sulfate moieties of GAGs brought about by morpholino-mediated knockdown of Hs6st show pleiotropic developmental phenotypes with most obvious effects on proper muscle formation in an intact *in vivo* model.

Acknowledgments—We thank S. van de Water and B. Schepman for technical assistence and J. Korving for histological sectioning. We thank the animal care facility for services rendered. We also thank the members of the Zivkovic, Den Hertog, and Van Eeden laboratories for helpful discussions and J. Bakkers for critically reading the manuscript.

REFERENCES

1. Esko, J. D., and Selleck, S. B. (2002) *Annu. Rev. Biochem.* **71,** 435–471
2. Perrimon, N., and Bernfield, M. (2000) *Nature* **404,** 725–728
3. Itoh, K., and Sokol, S. Y. (1994) *Development* **120,** 2703–2711
4. Wang, L., and Denburg, J. L. (1992) *Neuron* **8,** 701–714
5. Walz, A., McFarlane, S., Brickman, Y. G., Nurcombe, V., Bartlett, P. F., and Holt, C. E. (1997) *Development* **124,** 2421–2430
6. Irie, A., Yates, E. A., Turnbull, J. E., and Holt, C. E. (2002) *Development* **129,** 61–70
7. Topczewski, J., Sepich, D. S., Myers, D. C., Walker, C., Amores, A., Lele, Z., Hammerschmidt, M., Postlethwait, J., and Solnica-Krezel, L. (2001) *Dev. Cell* **1,** 251–264
8. Hacker, U., Lin, X., and Perrimon, N. (1997) *Development* **124,** 3565–3573
9. Lin, X., Buff, E. M., Perrimon, N., and Michelson, A. M. (1999) *Development* **126,** 3715–3723

10. Bellaiche, Y., The, I., and Perrimon, N. (1998) *Nature* **394,** 85–88
11. Lin, X., Wei, G., Shi, Z., Dryer, L., Esko, J. D., Wells, D. E., and Matzuk, M. M. (2000) *Dev. Biol.* **224,** 299–311
12. The, I., Bellaiche, Y., and Perrimon, N. (1999) *Mol. Cell* **4,** 633–639
13. Dhoot, G. K., Gustafsson, M. K., Ai, X., Sun, W., Standiford, D. M., and Emerson, C. P. J. (2001) *Science* **293,** 1663–1666
14. Bullock, S. L., Fletcher, J. M., Beddington, R. S., and Wilson, V. A. (1998) *Genes Dev.* **12,** 1894–1906
15. Ringvall, M., Ledin, J., Holmborn, K., van Kuppevelt, T., Ellin, F., Eriksson, I., Olofsson, A. M., Kjellen, L., and Forsberg, E. (2000) *J. Biol. Chem.* **275,** 25926–25930
16. Westerfield, M. (1994) *The Zebrafish Book*, University of Oregon Press, Eugene, OR
17. Delfert, D. M., and Conrad, H. E. (1985) *Anal. Biochem.* **148,** 303–310
18. Nasevicius, A., and Ekker, S. C. (2000) *Nat. Genet.* **26,** 216–220
19. Geisler, R., Rauch, G. J., Baier, H., van Bebber, F., Brobeta, L., Dekens, M. P., Finger, K., Fricke, C., Gates, M. A., Geiger, H., Geiger-Rudolph, S., Gilmour, D., Glaser, S., Gnugge, L., Habeck, H., Hingst, K., Holley, S., Keenan, J., Kirn, A., Knaut, H., Lashkari, D., Maderspacher, F., Martyn, U., Neuhauss, S., and Haffter, P. (1999) *Nat. Genet.* **23,** 86–89
20. Hammerschmidt, M., Pelegri, F., Mullins, M. C., Kane, D. A., van Eeden, F. J., Granato, M., Brand, M., Furutani-Seiki, M., Haffter, P., Heisenberg, C. P., Jiang, Y. J., Kelsh, R. N., Odenthal, J., Warga, R. M., and Nusslein-Volhard, C. (1996) *Development* **123,** 95–102
21. Lele, Z., Folchert, A., Concha, M., Rauch, G. J., Geisler, R., Rosa, F., Wilson, S. W., Hammerschmidt, M., and Bally-Cuif, L. (2002) *Development* **129,** 3281–3294
22. Kusche, M., Oscarsson, L. G., Reynertson, R., Roden, L., and Lindahl, U. (1991) *J. Biol. Chem.* **266,** 7400–7409
23. Habuchi, H., Tanaka, M., Habuchi, O., Yoshida, K., Suzuki, H., Ban, K., and Kimata, K. (2000) *J. Biol. Chem.* **275,** 2859–2868
24. Kjellen, L., and Lindahl, U. (1991) *Annu. Rev. Biochem.* **60,** 443–475
25. Lele, Z., Bakkers, J., and Hammerschmidt, M. (2000) *Genesis* **30,** 190–194
26. Ekker, S. C., and Larson, J. D. (2001) *Genesis* **30,** 89–93
27. Baeuerle, P. A., and Huttner, W. B. (1986) *Biochem. Biophys. Res. Commun.* **141,** 870–877
28. Humphries, D. E., and Silbert, J. E. (1988) *Biochem. Biophys. Res. Commun.* **154,** 365–371
29. Safaiyan, F., Kolset, S. O., Prydz, K., Gottfridsson, E., Lindahl, U., and Salmivirta, M. (1999) *J. Biol. Chem.* **274,** 36267–36273
30. Rudnicki, M. A., Schnegelsberg, P. N., Stead, R. H., Braun, T., Arnold, H. H., and Jaenisch, R. (1993) *Cell* **75,** 1351–1359
31. Weinberg, E. S., Allende, M. L., Kelly, C. S., Abdelhamid, A., Murakami, T., Andermann, P., Doerre, O. G., Grunwald, D. J., and Riggleman, B. (1996) *Development* **122,** 271–280
32. Muller, M., Weizsacker, E., and Campos-Ortega, J. A. (1996) *Development* **122,** 2071–2078
33. Haddon, C., Smithers, L., Schneider-Maunoury, S., Coche, T., Henrique, D., and Lewis, J. (1998) *Development* **125,** 359–370
34. Oates, A. C., and Ho, R. K. (2002) *Development* **129,** 2929–2946
35. Holley, S. A., Julich, D., Rauch, G. J., Geisler, R., and Nusslein-Volhard, C. (2002) *Development* **129,** 1175–1183
36. Westin, J., and Lardelli, M. (1997) *Dev. Genes Evol.* **207,** 51–63
37. Nomura-Kitabayashi, A., Takahashi, Y., Kitajima, S., Inoue, T., Takeda, H., and Saga, Y. (2002) *Development* **129,** 2473–2481
38. Sawada, A., Fritz, A., Jiang, Y., Yamamoto, A., Yamasu, K., Kuroiwa, A., Saga, Y., and Takeda, H. (2000) *Development* **127,** 1691–1702
39. Durbin, L., Sordino, P., Barrios, A., Gering, M., Thisse, C., Thisse, B., Brennan, C., Green, A., Wilson, S., and Holder, N. (2000) *Development* **127,** 1703–1713
40. Xu, Y., He, J., Wang, X., Lim, T. M., and Gong, Z. (2000) *Dev. Dyn.* **219,** 201–215
41. Devoto, S. H., Melancon, E., Eisen, J. S., and Westerfield, M. (1996) *Development* **122,** 3371–3380
42. Coutelle, O., Blagden, C. S., Hampson, R., Halai, C., Rigby, P. W., and Hughes, S. M. (2001) *Dev. Biol.* **236,** 136–150
43. Ekker, M., Wegner, J., Akimenko, M. A., and Westerfield, M. (1992) *Development* **116,** 1001–1010
44. Fjose, A., Njolstad, P. R., Nornes, S., Molven, A., and Krauss, S. (1992) *Mech. Dev.* **39,** 51–62
45. Yan, Y. L., Hatta, K., Riggleman, B., and Postlethwait, J. H. (1995) *Dev. Dyn.* **203,** 363–376
46. Lele, Z., and Krone, P. H. (1997) *Mech. Dev.* **61,** 89–98
47. Currie, P. D., and Ingham, P. W. (1996) *Nature* **382,** 452–455
48. Blagden, C. S., Currie, P. D., Ingham, P. W., and Hughes, S. M. (1997) *Genes Dev.* **11,** 2163–2175
49. Lewis, K. E., Currie, P. D., Roy, S., Schauerte, H., Haffter, P., and Ingham, P. W. (1999) *Dev. Biol.* **216,** 469–480
50. Krauss, S., Concordet, J. P., and Ingham, P. W. (1993) *Cell* **75,** 1431–1444
51. Concordet, J. P., Lewis, K. E., Moore, J. W., Goodrich, L. V., Johnson, R. L., Scott, M. P., and Ingham, P. W. (1996) *Development* **122,** 2835–2846
52. Habuchi, H., Kobayashi, M., and Kimata, K. (1998) *J. Biol. Chem.* **273,** 9208–9213
53. Zhang, L., Beeler, D. L., Lawrence, R., Lech, M., Liu, J., Davis, J. C., Shriver, Z., Sasisekharan, R., and Rosenberg, R. D. (2001) *J. Biol. Chem.* **276,** 42311–42321
54. Kamimura, K., Fujise, M., Villa, F., Izumi, S., Habuchi, H., Kimata, K., and Nakato, H. (2001) *J. Biol. Chem.* **276,** 17014–17021
55. Braat, A. K., van de Water, S., Korving, J., and Zivkovic, D. (2001) *Genesis* **30,** 183–185
56. van der Sar, A. M., Zivkovic, D., and den Hertog, J. (2002) *Dev. Dyn.* **223,** 292–297
57. Heasman, J. (2002) *Dev. Biol.* **243,** 209–214
58. Halfter, W., Schurer, B., Yip, J., Yip, L., Tsen, G., Lee, J. A., and Cole, G. J. (1997) *J. Comp. Neurol.* **383,** 1–17
59. Karthikeyan, L., Flad, M., Engel, M., Meyer-Puttlitz, B., Margolis, R. U., and Margolis, R. K. (1994) *J. Cell Sci.* **107,** 3213–3222
60. Becker, C. G., and Becker, T. (2002) *J. Neurosci.* **22,** 842–853
61. Holley, S. A., Geisler, R., and Nusslein-Volhard, C. (2000) *Genes Dev.* **14,** 1678–1690
62. Jiang, Y. J., Aerne, B. L., Smithers, L., Haddon, C., Ish-Horowicz, D., and Lewis, J. (2000) *Nature* **408,** 475–479
63. Florini, J. R., and Magri, K. A. (1989) *Am. J. Physiol.* **256,** 701–711
64. Hirsinger, E., Jouve, C., Malapert, P., and Pourquie, O. (1998) *Mol. Cell. Endocrinol.* **140,** 83–87
65. Rawls, A., and Olson, E. N. (1997) *Cell* **89,** 5–8
66. Olguin, H., and Brandan, E. (2001) *Dev. Dyn.* **221,** 106–115
67. Fuentealba, L., Carey, D. J., and Brandan, E. (1999) *J. Biol. Chem.* **274,** 37876–37884
68. Cossu, G., and Borello, U. (1999) *EMBO* **24,** 6867–6872
69. Ridgeway, A. G., Petropoulos, H., Wilton, S., and Skerjanc, I. S. (2000) *J. Biol. Chem.* **275,** 32398–32405
70. Petropoulos, H., and Skerjanc, I. S. (2002) *JBC* **277,** 15393–153999
71. Bradley, R. S., and Brown, A. M. (1990) *EMBO J.* **9,** 1569–1575
72. Reichsman, F., Smith, L., and Cumberledge, S. (1996) *J. Cell Biol.* **135,** 819–827
73. Binari, R. C., Staveley, B. E., Johnson, W. A., Godavarti, R., Sasisekharan, R., and Manoukian, A. S. (1997) *Development* **124,** 2623–2632
74. Blair, S. S. (2001) *Sci. STKE* **101,** 1–3
75. Giraldez, A. J., Copley, R. R., and Cohen, S. M. (2002) *Dev. Cell* **2,** 667–676
76. Hoppler, S., Brown, J. D., and Moon, R. T. (1996) *Genes Dev.* **10,** 2805–2817
77. McGrew, L. L., Takemaru, K., Bates, R., and Moon, R. T. (1999) *Mech. Dev.* **87,** 21–32
78. Lin, X., and Perrimon, N. (1999) *Nature* **400,** 281–284
79. Toyoda, H., Kinoshita-Toyoda, A., Fox, B., and Selleck, S. B. (2000) *J. Biol. Chem.* **275,** 21856–21861
80. Yip, G. W., Ferretti, P., and Copp, A. J. (2002) *Development* **129,** 2109–2119
81. Bulow, H. E., Berry, K. L., Topper, L. H., Peles, E., and Hobert, O. (2002) *Proc. Natl. Acad. Sci. U. S. A.* **99,** 6346–6351]